

Learning to Walk via Deep Reinforcement Learning

Tuomas Haarnoja*
Google, UC Berkeley

Sehoon Ha*
Google

Aurick Zhou
UC Berkeley

Jie Tan
Google

George Tucker
Google

Sergey Levine
Google, UC Berkeley

Abstract—Deep reinforcement learning offers the promise of automatic acquisition of robotic control policies that directly map sensory inputs to low-level actions. In the domain of robotic locomotion, it could make it possible for locomotion skills to be learned with minimal engineering and without even needing to construct a model of the robot. However, applying deep reinforcement learning methods on real-world robots is exceptionally difficult, due both to the sample complexity and, just as importantly, the sensitivity of such methods to hyperparameters. While hyperparameter tuning can be performed in parallel in simulated domains, it is usually impractical to tune hyperparameters directly on real-world robotic platforms, especially legged platforms like quadrupedal robots that can be damaged through extensive trial-and-error learning. We develop a stable deep RL algorithm that extends soft actor-critic, requires minimal hyperparameter tuning, and requires only a modest number of trials to learn multilayer neural network policies. We then apply this method to learn walking gaits on a real-world Minitaur robot. Our method can learn to walk from scratch directly in the real world in two hours of training, without any model or simulation, and the resulting policy is robust to moderate variations in the environment. We further show that our algorithm achieves state-of-the-art performance on four standard simulated benchmarks.

I. INTRODUCTION

Designing locomotion controllers for legged robots is a long-standing research challenge. Current state-of-the-art methods typically employ a pipelined approach, consisting of components such as state estimation, contact scheduling, trajectory optimization, foot placement planning, model-predictive control, and operational space control [12, 22, 4, 2]. Designing these components requires expertise, and often an accurate dynamic model of the robot that can be difficult to acquire. In contrast, end-to-end deep reinforcement learning does not assume any prior knowledge of the gait or the robot’s dynamics, which in principle should make it feasible to apply directly to robotic systems without any explicit state identification or manual engineering. Such an end-to-end method could automate locomotion controller design, completely removing the need for system identification and creating gaits that are very well adapted to the particular robot and its environment. However, applying deep reinforcement learning to learn gaits in the real world is challenging, since current algorithms often require a large number of samples – on the order of tens of thousands of trials [41]. Furthermore, such algorithms are often highly sensitive to hyperparameter settings, and require considerable tuning [20], which is infeasible in the real world. For this reason, many prior methods have studied learning of locomotion

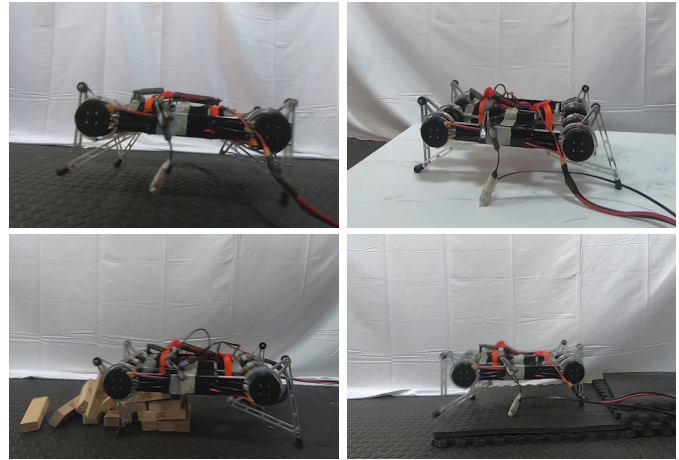


Fig. 1: Illustration of a walking gait learned in the real world. The policy is trained only on flat terrain, but due to maximum entropy training, the learned gait is stable and robust, and enables the robot to traverse obstacles that were not seen during training.

gaits in simulation [19, 45, 32, 3], which still requires system identification and modeling.

In this paper, we aim to address these challenges by developing an efficient deep reinforcement learning algorithm that is less sensitive to the choice of hyperparameters, and thereby devise a method that can be used to learn locomotion gaits directly in the real world, with no prior modeling. In particular, we extend the framework of maximum entropy reinforcement learning. Methods of this type, such as soft actor-critic [17] and soft Q-learning [14], can achieve state-of-the-art sample efficiency [17] and have been successfully deployed for other real-world tasks, such as robotic manipulation, where they exhibit a high degree of robustness due to entropy maximization [16]. However, maximum entropy RL algorithms are sensitive to the choice of temperature parameter, which determines the trade-off between exploration (the entropy weight) and exploitation (reward maximization). In practice, this temperature is a hyperparameter that must be tuned manually.

We devise a variant of the maximum entropy soft actor-critic algorithm [17] that removes the need to manually tune the temperature, proposing a simple and automatic gradient-based temperature tuning method that adjusts the expected entropy over the visited states to match a target value. In contrast to standard reinforcement learning, our method only controls the expected entropy over states, while the per-state entropy can still vary—a desirable property that allows the

*Equal contribution, haarnoja@berkeley.edu, sehoonha@google.com

policy to automatically reduce entropy for states where acting deterministically is preferred, while still acting stochastically in other states. Consequently, it virtually eliminates the need for per-task hyperparameter tuning, making it practical for us to apply this algorithm to learn quadrupedal locomotion gaits directly on a real-world robotic system.

The principal contribution of our paper is an end-to-end reinforcement learning framework for legged locomotion on real robots, which includes a data efficient learning algorithm based on maximum entropy reinforcement learning and an asynchronous learning system on the real robots. It enables a Minitaur [25] robot (Figure 1) to learn to walk automatically. While the training is conducted on a flat ground, the learned policy can generalize to unseen terrains and is moderately robust to perturbations. The training requires about 400 rollouts, equivalent to two hours. In addition to the robot experiments, we conduct a comprehensive evaluation of our algorithm on simulated benchmark tasks, where we show that our method achieves state-of-the-art performance and, unlike prior works based on maximum entropy RL, can use exactly the same hyperparameters for all tasks.

II. RELATED WORK

Current state-of-the-art locomotion controllers typically adopt a pipelined control scheme. For example, the MIT Cheetah [4] uses a state machine over contact conditions, then generates simple reference trajectories, performs model predictive control [8] to plan for desired contact forces, and then uses Jacobian transpose control to realize them. The ANYmal robot [22] plans footholds based on the inverted pendulum model [35], applies CMA-ES [18] to optimize a parametrized controller [11, 12], and solves a hierarchical operational space control problem [21] to produce joint torques, contact forces, and body motion. While these methods can provide effective gaits, they require considerable prior knowledge of the details of the locomotion task and, more importantly, a characterization of the robot’s dynamics. In contrast, our method aims to control the robot without prior knowledge of either the gait or the robot’s dynamics. We do not assume access to any trajectory design, foothold planner, or a dynamics model of the robot, since all learning is done entirely through real-world interaction. The only requirement is knowledge of the state and action space, which in our implementation corresponds to joint angles, IMU readings, and desired motor positions. While in practice, access to additional prior knowledge could be used to accelerate learning (see, e.g., [24]), end-to-end methods that make minimal prior assumptions are broadly applicable, and developing such techniques will make it more scalable to acquire gaits for diverse robots in diverse conditions.

Deep reinforcement learning has been used extensively to learn locomotion policies in simulation [19, 45, 32, 3] and even transfer them to real-world robots [41, 23], but this inevitably incurs some loss of performance due to discrepancies in the simulation, and requires accurate system identification. Using such algorithms directly in the real world has proven challenging. Real-world applications typically make use of

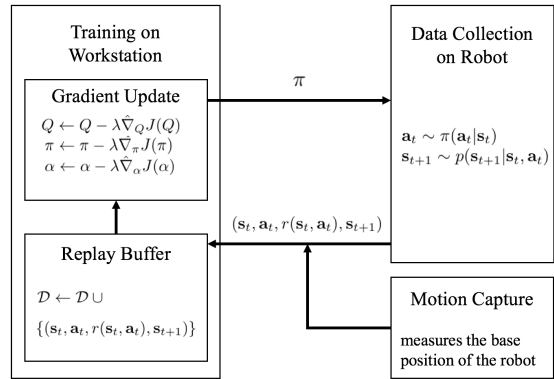


Fig. 2: Overview of our asynchronous learning system. The learning system runs the training and data collection asynchronously and seamlessly across multiple machines.

simple and inherently stable robots [13] or low-dimensional gait parameterizations [28, 7, 34], or both [42]. In contrast, we show we can acquire locomotion skills directly in the real world using policies based on deep neural networks.

Our algorithm is based on maximum entropy reinforcement learning, which maximizes both the expected return and the expected entropy of the policy. This framework has been used in many contexts, from inverse reinforcement learning [46] to optimal control [43, 44, 36]. One advantage of this framework is that it produces relatively robust policies, since noise injection during training causes the policy to learn to handle perturbations, analogously to robust control. However, the weight on the entropy term (the “temperature”) is typically chosen heuristically [31, 14, 30, 38, 17]. As we observe in our experiments, this parameter is very sensitive in practice, and tuning it by hand can make real-world application of this framework difficult. We propose to instead constrain the expected entropy of the policy, and adjust the temperature automatically to satisfy this constraint. This constraint is related in spirit to KL-divergence constraints that limit the policy *change* between iterations [33, 37, 1], but is applied directly to the current policy’s entropy. We find that this simple modification drastically reduces the amount of parameter tuning that is required, both on benchmark problems and our robotic locomotion task.

III. ASYNCHRONOUS LEARNING SYSTEM

We first describe our asynchronous robotic reinforcement learning system, which we will use to evaluate real-world reinforcement learning for robotic locomotion. The system, shown in Figure 2, consists of three components: a data collection job that collects the robot data, a motion capture job that computes the reward signal based on the robot’s position, as measured by motion capture, and a training job that updates the neural networks. These subsystems run asynchronously on different machines. When the learning system starts, these components are synchronized to a common clock and use timestamps to sync the future data streams.

The data collection job runs on the onboard computer of the

robot, which executes the latest policy π that is pushed from the training job. For each control step t , it collects observations s_t , performs neural network policy inference and executes the actions a_t . The entire trajectory of the rollout is recorded into tuples $(s_t, a_t, s_{t+1})_{t=0, \dots, N-1}$ and sent back to the training job. The motion capture system measures the position of the robot and provides the reward signal r for reinforcement learning. The training subsystem runs on a workstation. It periodically pulls data from the robot and the motion capture system, evaluate the reward function, and appends the into a replay buffer, which is used by the reinforcement learning algorithm. At each iteration of training, the training job randomly samples a batch of data from this buffer, and uses stochastic gradient descent to update the value network, the policy network, and the temperature parameter, as we will discuss in Section V. Once the training is started, minimal human intervention is needed, except for the need to reset the robot if it falls or walks too far from its initial position.

The asynchronous design minimizes the training time by amortizing data collection and training costs across different machines. More importantly, we can pause or restart any subsystem seamlessly without affecting the other subsystems. In practice, we found this particularly useful because we often encounter hardware and communication errors, in which case we can safely restart the subsystem without negatively impact the learning process. Our system could in principle be scaled to multiple robots simply by increasing the number of data collection jobs.

IV. REINFORCEMENT LEARNING PRELIMINARIES

Reinforcement learning aims to learn a policy that maximizes the expected sum of rewards [40]. We consider infinite-horizon Markov decision processes where the state space \mathcal{S} and action space \mathcal{A} are continuous. The agent starts at an initial state $s_0 \sim p(s_0)$. Then, the agent repeatedly samples an action \mathbf{a}_t from a policy $\pi_\theta(\mathbf{a}_t|s_t)$, receives a bounded reward $r(s_t, \mathbf{a}_t)$, and transitions to a subsequent state s_{t+1} according to the Markovian dynamics $p(s_{t+1}|\mathbf{a}_t, s_t)$ of the environment. This generates a trajectory of states and actions $\tau = (s_0, \mathbf{a}_0, s_1, \mathbf{a}_1, \dots)$. We denote the trajectory distribution induced by π by $\rho_\pi(\tau)$, the state-action marginal by $\rho_\pi(s_t, \mathbf{a}_t)$ and the state marginal by $\rho_\pi(s_t)$.

Maximum entropy reinforcement learning optimizes both the expected return and the entropy of the policy. The corresponding objective can be expressed as

$$J(\pi) = \sum_{t=0}^T \mathbb{E}_{\tau \sim \rho_\pi} [r(s_t, \mathbf{a}_t) - \alpha \log \pi(\mathbf{a}_t|s_t)], \quad (1)$$

which incentivizes the policy to explore more widely and is more robust in practice [17]. The temperature parameter α determines the relative importance of the entropy term against the reward, and thus controls the stochasticity of the optimal policy. The maximum entropy objective differs from the standard maximum expected reward objective used in conventional reinforcement learning, though the conventional

objective can be recovered in the limit as $\alpha \rightarrow 0$. We can extend the objective to infinite horizon problems by introducing a discount factor γ to ensure that the sum of expected rewards and entropies is finite [14].

One of the central challenges with the objective in (1) is that the trade-off between maximizing the return, or exploitation, versus the entropy, or exploration, is directly affected by the scale of the reward function. Unlike in conventional reinforcement learning, where the optimal policy is independent of scaling of the reward function, in maximum entropy reinforcement learning the scaling factor has to be tuned per environment, and a sub-optimal scale can drastically degrade the performance [17].

V. AUTOMATING ENTROPY ADJUSTMENT FOR MAXIMUM ENTROPY RL

Learning robotic locomotion in the real world requires an algorithm that is efficient and relatively insensitive to hyperparameters, which are impractical to tune directly on a real-world platform. In this section, we describe our extension of maximum entropy reinforcement learning which enables automated temperature tuning, substantially reducing sensitivity to the temperature parameter. We will first derive a theoretical algorithm for finite horizon case, and then suggest a practical algorithm for discounted, infinite horizon case based on the theory.

Instead of requiring the user to set the temperature or reward scale¹ manually, we can automate this process by formulating a different maximum entropy reinforcement learning objective, where the entropy is treated as a constraint. The magnitude of the reward differs not only across tasks, but it also depends on the policy, which improves over time during training. Since the optimal entropy depends on this magnitude, this makes the temperature adjustment particularly difficult: the entropy can vary unpredictably both across tasks and during training as the policy becomes better. Simply forcing the entropy to a fixed value is a poor solution, since the policy should be free to explore more in regions where the optimal action is uncertain, but remain more deterministic in states with a clear distinction between good and bad actions. Instead, we formulate a constrained optimization problem where the *average* entropy of the policy is constrained, while the entropy at different states can vary. We show that the dual to this constrained optimization leads to the soft actor-critic updates [17], along with an additional update for the dual variable, which plays the role of the temperature. Our formulation also makes it possible to learn the entropy with more expressive policies that can model multi-modal distributions, such as policies based on normalizing flows [15], for which no closed form expression for the entropy exists.

A. Constrained Entropy Objective

Our aim is to find a stochastic policy with maximal expected return that satisfies a minimum expected entropy constraint.

¹Reward scale is the reciprocal of temperature. We will use these two terms interchangeably throughout this paper.

Formally, we want to solve the constrained optimization problem

$$\max_{\pi_{0:T}} \mathbb{E}_{\rho_\pi} \left[\sum_{t=0}^T r(\mathbf{s}_t, \mathbf{a}_t) \right] \text{ s.t. } \mathbb{E}_{\rho_\pi} [-\log(\pi_t(\cdot | \mathbf{s}_t))] \geq \mathcal{H}, \quad (2)$$

where \mathcal{H} is a desired minimum expected entropy. Note that, for fully observed MDPs, the policy that optimizes the expected return is deterministic, so we expect this constraint to usually be tight and do not need to impose an upper bound on the entropy.

Since the policy at time t can only affect the future objective value, we can employ an (approximate) dynamic programming approach, solving for the policy backward through time. We rewrite the objective as an iterated maximization

$$\max_{\pi_0} \left(\mathbb{E} [r(\mathbf{s}_0, \mathbf{a}_0)] + \max_{\pi_1} \left(\mathbb{E} [\dots] + \max_{\pi_T} \mathbb{E} [r(\mathbf{s}_T, \mathbf{a}_T)] \right) \right),$$

subject to the constraint on entropy. Starting from the last time step, we change the constrained maximization to the dual problem. Subject to $\mathbb{E}_{\rho_\pi} [-\log(\pi_T(\cdot | \mathbf{s}_T))] \geq \mathcal{H}$,

$$\begin{aligned} \max_{\pi_T} \mathbb{E}_{(\mathbf{s}_T, \mathbf{a}_T) \sim \rho_\pi} [r(\mathbf{s}_T, \mathbf{a}_T)] = \\ \min_{\alpha_T \geq 0} \max_{\pi_T} \mathbb{E} [r(\mathbf{s}_T, \mathbf{a}_T) - \alpha_T \log \pi(\mathbf{a}_T | \mathbf{s}_T)] - \alpha_T \mathcal{H}, \end{aligned}$$

where α_T is the dual variable. We have also used strong duality, which holds since the objective is linear and the constraint (entropy) is a convex function in π_T . This dual objective is closely related to the maximum entropy RL objective with respect to the policy. Let $\pi_T^*(\mathbf{a}_T | \mathbf{s}_T; \alpha_T)$ be the unique maximizer. We can solve for the optimal dual variable α_T^* as

$$\arg \min_{\alpha_T} \mathbb{E}_{\mathbf{s}_T, \mathbf{a}_T \sim \pi_T^*} [-\alpha_T \log \pi_T^*(\mathbf{a}_T | \mathbf{s}_T; \alpha_T) - \alpha_T \mathcal{H}]. \quad (3)$$

To simplify notation, we make use of the recursive definition of the soft Q-function [14]

$$\begin{aligned} Q_t^*(\mathbf{s}_t, \mathbf{a}_t; \pi_{t+1:T}^*, \alpha_{t+1:T}^*) = \mathbb{E} [r(\mathbf{s}_t, \mathbf{a}_t)] + \\ \mathbb{E}_{\rho_\pi} [Q_{t+1}^*(\mathbf{s}_{t+1}, \mathbf{a}_{t+1}) - \alpha_{t+1}^* \log \pi_{t+1}^*(\mathbf{a}_{t+1} | \mathbf{s}_{t+1})], \end{aligned}$$

with $Q_T^*(\mathbf{s}_T, \mathbf{a}_T) = \mathbb{E} [r(\mathbf{s}_T, \mathbf{a}_T)]$. Now, subject to the entropy constraints and again using the dual problem, we have

$$\begin{aligned} \max_{\pi_{T-1}} \left(\mathbb{E} [r(\mathbf{s}_{T-1}, \mathbf{a}_{T-1})] + \max_{\pi_T} \mathbb{E} [r(\mathbf{s}_T, \mathbf{a}_T)] \right) = \\ \max_{\pi_{T-1}} \left(Q_{T-1}^*(\mathbf{s}_{T-1}, \mathbf{a}_{T-1}) - \alpha_T \mathcal{H} \right) = \\ \min_{\alpha_{T-1} \geq 0} \max_{\pi_{T-1}} \left(\mathbb{E} [Q_{T-1}^*(\mathbf{s}_{T-1}, \mathbf{a}_{T-1})] \right. \\ \left. - \mathbb{E} [\alpha_{T-1} \log \pi(\mathbf{a}_{T-1} | \mathbf{s}_{T-1})] - \alpha_{T-1} \mathcal{H} \right) + \alpha_T^* \mathcal{H}. \end{aligned}$$

In this way, we can proceed backwards in time and recursively optimize (2).

Maximizing over the terms that depend on π_t from the previous equation, the optimal policy $\pi_t^*(\mathbf{a}_t | \mathbf{s}_t; \alpha_t)$ for time t

is

$$\begin{aligned} \pi_t^* = \arg \max_{\pi_t} \mathbb{E} [Q_t^*(\mathbf{s}_t, \mathbf{a}_t) - \alpha_t \log \pi(\mathbf{a}_t | \mathbf{s}_t)] \\ = \arg \min_{\pi_t} \text{D}_{\text{KL}} \left(\pi_t \parallel \frac{1}{Z(\mathbf{s}_t)} \exp \left(\frac{1}{\alpha_t} Q_t^*(\mathbf{s}_t, \mathbf{a}_t) \right) \right), \end{aligned} \quad (4)$$

where $Z(\mathbf{s}_t) = \int \exp \left(\frac{1}{\alpha_t} Q_t^*(\mathbf{s}_t, \mathbf{a}_t) \right) d\mathbf{a}_t$ does not depend on π_t^* , so we can ignore it for the purposes of optimizing π_t^* . This is exactly the soft policy improvement step introduced by [17], with an additional temperature parameter α_t . In contrast to [17], which shows that this update leads to an improvement in the policy, we derived it directly starting from the objective function. Note that the optimal policy at time t is a function of the dual variable α_t^* . After solving for Q_t^* and π_t^* , we can minimize over the terms involving the dual variable α_t :

$$\alpha_t^* = \arg \min_{\alpha_t} \mathbb{E}_{\mathbf{a}_t \sim \pi_t^*} [-\alpha_t \log \pi_t^*(\mathbf{a}_t | \mathbf{s}_t; \alpha_t) - \alpha_t \mathcal{H}]. \quad (5)$$

The solutions in (4) and (5) constitute the core of our algorithm. In theory, exactly solving these equations recursively optimizes the entropy-constrained maximum expected return objective in (2). However, to produce a practical algorithm for real-world learning, we will need to utilize function approximators and stochastic gradient descent, as discussed in the next section.

B. Practical Algorithm

In practice, we cannot perform the optimization steps in (4) and (5) exactly. We instead parameterize a Gaussian policy with parameters ϕ and a temperature parameter, and learn the policy using stochastic gradient descent for the discounted, infinite horizon problem. We additionally use two parameterized Q-functions, with parameters θ_1 and θ_2 , as suggested in [17]. We learn the Q-function parameters as a regression problem by minimizing the following loss $J_Q(\theta_i)$:

$$\mathbb{E}_{(\mathbf{s}_t, \mathbf{a}_t, \mathbf{s}_{t+1}) \sim \mathcal{D}} \left[\left(Q_{\theta_i}(\mathbf{s}_t, \mathbf{a}_t) - (r(\mathbf{s}_t, \mathbf{a}_t) + \gamma V_{\theta_1, \theta_2}(\mathbf{s}_{t+1})) \right)^2 \right] \quad (6)$$

using minibatches from a replay buffer \mathcal{D} . The value function $V_{\theta_1, \theta_2}(\mathbf{s}_t)$ is implicitly defined through the Q-functions and the policy as $\mathbb{E}_{\mathbf{a}_t \sim \pi_\phi} \left[\min_{i \in \{1, 2\}} Q_{\theta_i}(\mathbf{s}_t, \mathbf{a}_t) - \alpha \log \pi_\phi(\mathbf{a}_t | \mathbf{s}_t) \right]$. We learn a Gaussian policy by minimizing

$$J_\pi(\phi) = \mathbb{E}_{\mathbf{s}_t \sim \mathcal{D}, \mathbf{a}_t \sim \pi_\phi} \left[\alpha \log \pi_\phi(\mathbf{a}_t | \mathbf{s}_t) - \min_{i \in \{1, 2\}} Q_{\theta_i}(\mathbf{s}_t, \mathbf{a}_t) \right], \quad (7)$$

using the reparameterization trick [27]. This procedure is the same as the standard soft actor-critic algorithm [17], but with an explicit, dynamic temperature α .

To learn α , we need to minimize the dual objective in (5). This can be done by approximating dual gradient descent [5]. Dual gradient descent alternates between optimizing the Lagrangian with respect to the primal variables to convergence, and then taking a gradient step on the dual variables. While optimizing with respect to the primal variables fully is impractical, a truncated version that performs incomplete optimization

(even a single gradient step) can be shown to converge under convexity assumptions [5]. While such assumptions do not apply to the case of nonlinear function approximators such as neural networks, we found this approach to still work in practice. Thus, we compute gradients for α with the following objective:

$$J(\alpha) = \mathbb{E}_{\mathbf{s}_t \sim \mathcal{D}, \mathbf{a}_t \sim \pi_\phi} [-\alpha \log \pi_\phi(\mathbf{a}_t | \mathbf{s}_t) - \alpha \mathcal{H}]. \quad (8)$$

The proposed algorithm alternates between a data collection phase and an optimization phase. In the optimization phase, the algorithm optimizes all objectives in (6) – (8) jointly. We also incorporate delayed target Q-function networks as is standard in prior work. Algorithm 1 summarizes the full algorithm, where $\hat{\nabla}$ denotes stochastic gradients.

Algorithm 1: Soft Actor-Critic with Automatic Entropy Adjustment

```

1 Initialize function approximators parameters  $\theta_1, \theta_2, \phi$ , and
  a global temperature coefficient  $\alpha$ .
2 for each iteration do
3   for each environment step do
4      $\mathbf{a}_t \sim \pi(\mathbf{a}_t | \mathbf{s}_t)$ 
5      $\mathbf{s}_{t+1} \sim p(\mathbf{s}_{t+1} | \mathbf{s}_t, \mathbf{a}_t)$ 
6      $\mathcal{D} \leftarrow \mathcal{D} \cup \{(\mathbf{s}_t, \mathbf{a}_t, r(\mathbf{s}_t, \mathbf{a}_t), \mathbf{s}_{t+1})\}$ .
7   end
8   for each gradient step do
9      $\theta_i \leftarrow \theta_i - \lambda \hat{\nabla}_{\theta_i} J_Q(\theta_i)$  for  $i \in \{1, 2\}$ 
10     $\phi \leftarrow \phi - \lambda \hat{\nabla}_{\phi} J_{\pi}(\phi)$ 
11     $\alpha \leftarrow \alpha - \lambda \hat{\nabla}_{\alpha} J(\alpha)$ 
12  end
13   $\bar{\theta}_i \leftarrow \tau \theta_i + (1 - \tau) \bar{\theta}_i$  for  $i \in \{1, 2\}$ 
14 end

```

VI. EVALUATION ON SIMULATION ENVIRONMENTS

Before evaluating our method on real-world locomotion, we conduct a comprehensive evaluation in simulation to validate our learning algorithm. Our goal is to answer following four questions:

- 1) Does our method achieve the state-of-the-art data efficiency?
- 2) How sensitive is our method to the hyperparameter settings?
- 3) Is our method effectively regulating the entropy and dynamically adjusting the temperature during learning?
- 4) Can the learned locomotion policy generalize to unseen situations?

A. Evaluation on OpenAI Benchmark Environments

To answer above questions, we first evaluate our algorithm on four standard benchmark environments for continuous locomotion tasks in OpenAI Gym benchmark suite [6], ranging from HalfCheetah with six action dimensions to Humanoid with 17-dimensional actions. We compare our method to soft actor-critic (SAC) [17] with a fixed temperature parameter

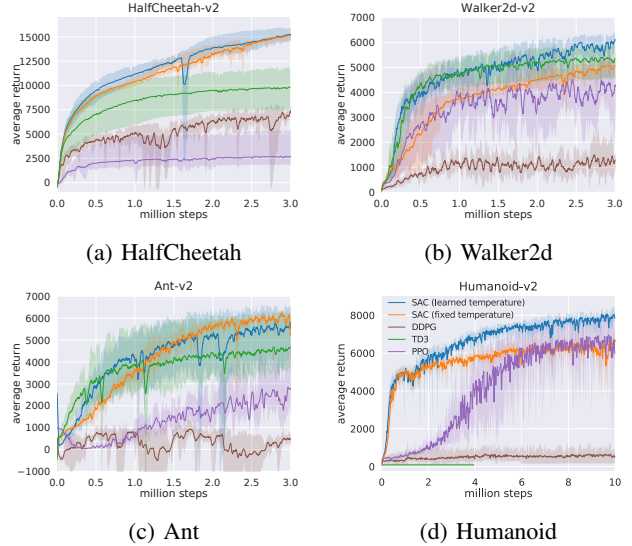
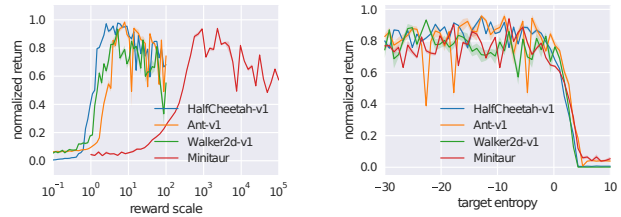


Fig. 3: (a) – (d) Standard benchmark training results. Our method (blue) achieves similar or better performance compared to other algorithms. Note that all other algorithms except ours went through dense hyperparameter tuning to achieve the above learning curves.



(a) Standard SAC over reward scale (b) Our method over target entropy

Fig. 4: Average normalized performance over the last 100k samples on a range of environments. (a) Performance of standard SAC as a function of reward scale, and (b) Performance of our method as a function of target entropy. Our method is substantially less sensitive to the choice of the hyper-parameter controlling the stochasticity of the policy.

that is tuned for each environment. We also compare to deep deterministic policy gradient (DDPG) [29], proximal policy optimization (PPO) [39], and twin delayed deep deterministic policy gradient algorithm (TD3) [10]. All of the algorithms use the same network architecture: all of the function approximators (policy and Q-functions for SAC) are parameterized with a two-layer neural network with 256 hidden units on each layer, and we use ADAM [26] with the same learning rate of 0.0003 to train all the networks and temperature parameter α . For standard SAC, we tune the reward scale per environment using grid search. Poorly chosen reward scales can degrade performance drastically (see Figure 4a). For our method, we simply set the target entropy to be -1 per action dimension (i.e., HalfCheetah has target entropy -6, while Humanoid uses -17).

1) *Comparative Evaluation:* Figure 3(a) – (d) show a comparison of the algorithms. The solid line denotes the average performance over 5 random seeds, and the shaded region corresponds to the best and worst performing seeds. The results indicate that our method (blue) achieves practically

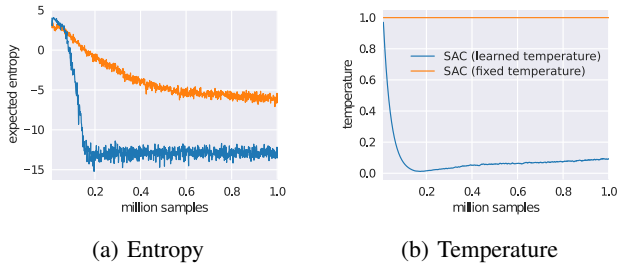


Fig. 5: Comparison of our method and standard SAC in terms of entropy and temperature on HalfCheetah. The target entropy for learning the temperature of SAC is -13 in this case.

identical or better performance compared to standard SAC (orange), which is tuned per environment for all environments. Overall, our method performs better or comparably to the other baselines, standard SAC, DDPG, TD3, and PPO.

2) *Sensitivity Analysis*: We compare the sensitivity to the hyperparameter between our method (target entropy) and the standard SAC (reward scale). Both maximum entropy RL algorithms [17] and standard RL algorithms [20] can be very sensitive to the scale of the reward function. In the case of maximum entropy RL, this scale directly affects the trade-off between reward maximization and entropy maximization [17]. We first validate the sensitivity of standard SAC by running experiments on the HalfCheetah, Walker, Ant, and the simulated Minitaur robot (See Section VI-B for more details). Figure 4a shows the returns for a range of reward scale values that are normalized to the maximum reward of the given task. All benchmark environments achieve good performance for about the same range of values, between 1 to 10. On the other hand, the simulated Minitaur requires roughly two orders of magnitude larger reward scale to work properly. This result indicates that, while standard benchmarks offer high variability in terms of task dimensionality, they are homogeneous in terms of other characteristics, and testing only on the benchmarks might not generalize well to seemingly similar tasks designed for different purposes. This suggests that the good performance of our method, with the same hyperparameters, on both the benchmark tasks and the Minitaur task accurately reflects its generality and robustness. Figure 4b compares the sensitivity of our method to the target entropy value on the same set of tasks. In this case, the range of good target entropy values is essentially the same for all environments, making hyperparameter tuning substantially less laborious. It is also worth noting that this range is large, suggesting that our algorithm is relatively insensitive to the choice of this hyperparameter.

3) *Validation of Entropy Control*: Next, we compared how the entropy and temperature evolve during training. Figure 5a compares the entropy (estimated as an expected negative log probability over a minibatch) on HalfCheetah for SAC with fixed temperature (orange) and our method (blue), which uses a target entropy of -13. The figure clearly indicates that our algorithm is able to match the target entropy in a relatively small number of steps. On the other hand, regular SAC has

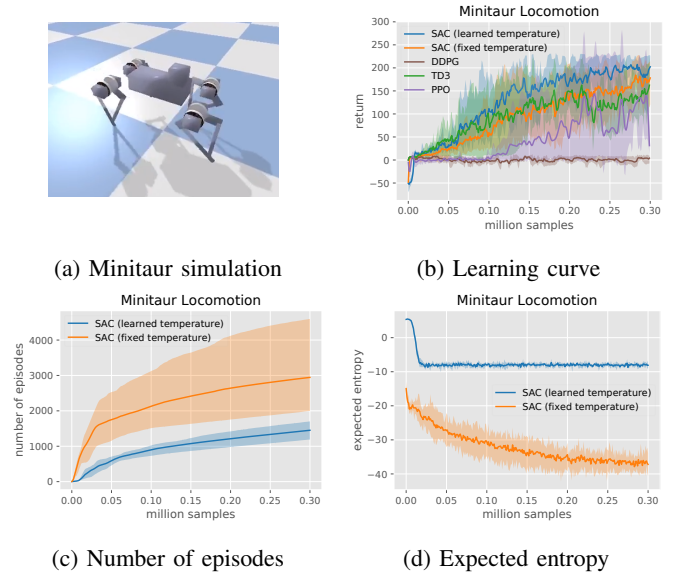


Fig. 6: (a) Illustration of the Minitaur environment. (b) Learning curves for the Minitaur environment. For our method (blue), we used exactly the same hyper-parameters as we used for the benchmarks whereas for the baseline (orange), we needed to tune the reward scale. (c) Number of episodes during training. (d) Expected entropy during training.

a fixed temperature parameter and thus the entropy slowly decreases as the Q-function increases. Figure 5b compares the temperature parameter of the two methods. Our method (blue) actively adjusts the temperature, particularly in the beginning of training when the Q-values are small and the entropy term dominates in the objective. The temperature is quickly pulled down so as to make the entropy to match the target. For other simulated environments, we observed similar entropy and temperature curves throughout the learning.

B. Evaluation on Simulated Minitaur Environment

Next, we evaluate our method on a simulated Minitaur locomotion tasks (Figure 6.) Simulation allows us to quantify perturbation robustness, measure states that are not accessible on the robot, and more importantly, gather more data point to evaluate our algorithm. To prevent bias of our conclusion, we have also conducted a careful system identification, following Tan et al. [41], such that our simulated robot is moderately representative of the real system. However, we emphasize that, in this work, we do not transfer any simulated policy to the real world directly – all real-world experiments use only real-world training, without access to any simulator or model.

Figure 6b compares the learning curve of our method to the state-of-the-art deep reinforcement learning algorithms. Our method is the most data efficient. Note that in order to obtain the result of SAC (fixed temperature) in the plot, we had to sweep through a set of candidate temperatures and choose the best one. This mandatory hyperparameter tuning is equivalent to collecting an order of magnitude more samples, which is not shown in Figure 6b. While the *number of steps* is a common measure of data efficiency in the learning community, the *number of episodes* can be another important indicator

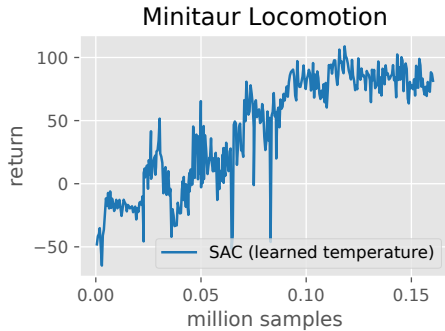


Fig. 7: Learning curve of SAC with learned temperature on the Minitaur robot.

for robotics because the number of episodes determines the number of experiment reset, which typically is time-consuming and require human intervention. Figure 6c indicates that our method takes fewer numbers of episodes for training a good policy. In the experiments, our algorithm effectively escapes a local minimum of “diving forward”, which is a common cause of falling and early episode termination, by maintaining the policy entropy at higher values (Figure 6d).

The final learned policy in simulation qualitatively resembles the gait learned directly on the robots. We tested its robustness by applying lateral perturbations to its base for 0.5 seconds with various magnitudes. Even though no perturbation is injected during training, the simulated robot can withstand up to 220N lateral pushes and subsequently recover to normal walking. This is significantly larger than the maximum 130N of the best PPO-trained policy that is picked out of 1000 learning trials. We suspect that this robustness emerges automatically from the SAC method due to entropy maximization at training time.

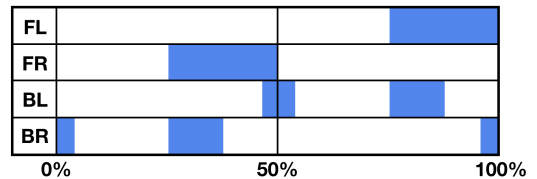
VII. LEARNING IN THE REAL WORLD

In this section, we describe the real-world learning experiments on the Minitaur robot. We aim to answer the following questions:

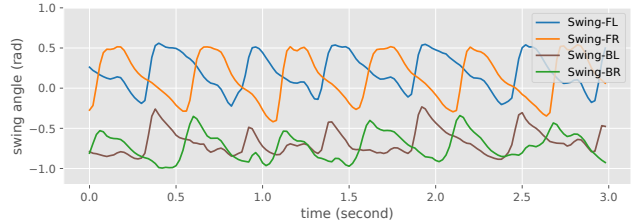
- 1) Can our method efficiently train a policy on hardware without hyper-parameter tuning?
- 2) Can the learned policy generalize to unseen situations?

A. Experiment Setup

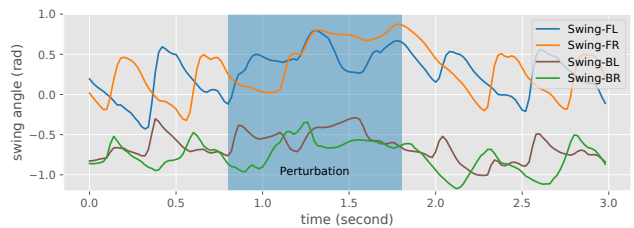
Quadrupedal locomotion presents substantial challenges for real-world reinforcement learning. The robot is underactuated, and must therefore delicately balance contact forces on the legs to make forward progress. A suboptimal policy can cause it to lose balance and fall, which will quickly damage the hardware, making sample-efficient learning essential. In this section, we test our learning method and system on a quadrupedal robot in the real world settings. We use the Minitaur robot, a small-scale quadruped with eight direct-drive actuators [25]. Each leg is controlled by two actuators that allow it to move in the sagittal plane. The Minitaur is equipped with motor encoders that measure the motor angles and an IMU that measures the orientation and angular velocity of Minitaur’s base.



(a) Footfall pattern of learned gait



(b) Swing angles of learned gait



(c) Swing angles of learned gait with perturbations

Fig. 8: Illustration of the learned policy. (a) Footfall pattern of a single cycle of the learned gait. Swing phases are drawn as blue bars. (b) Swing angles of four legs, which are periodic and synchronized. (c) Swing angles with an external perturbation. The learned policy successfully recovers to the nominal gait.

In our MDP formulation, the observation includes eight motor angles, the roll angle, velocity, the pitch angle and velocity of the base. We choose to exclude the yaw measurement because it drifts quickly. The action space includes the swing angle and the extension of each leg, which are then mapped to desired motor positions and tracked with a PD controller [41]. Because the Minitaur robot does not support direct torque control, which is more suitable for locomotion, we choose low PD gains $k_p = 0.3$ and $k_d = 0.003$ to ensure compliant motion. We find that the latencies in the hardware and the partial observation make the system non-Markovian, which significantly degrades the learning performance. We therefore augment an observation space to include a history of the last five observations and actions which results in a 112 dimensional observation space. The reward function encourages longer walking distance, which is measured using the motion capture system, and penalizes large joint accelerations, computed via finite differences using the last three actions. We also find it necessary to penalize large pitch angle of the base and the joint angles when the front legs are folded under the robot, which is the most common failure case that require manual resets. We parameterize the policy and the value functions with fully connected feed-forward neural networks with two hidden-layers and 256 neurons per layer, which are randomly initialized.

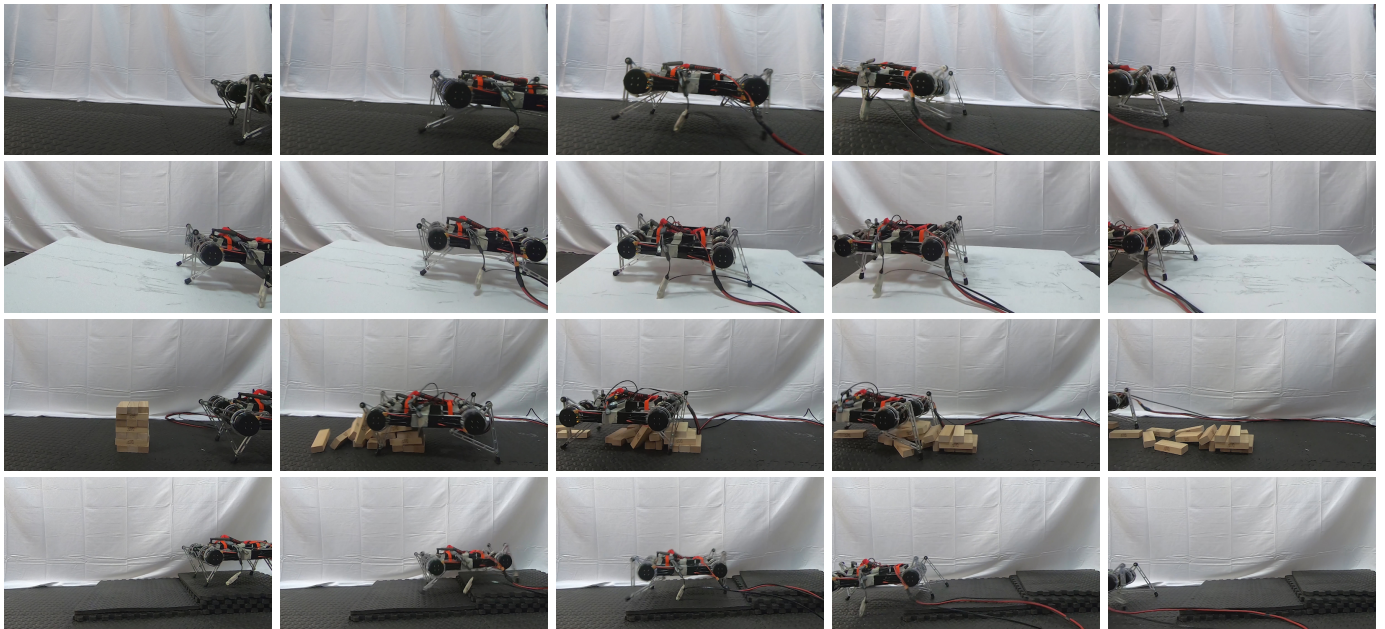


Fig. 9: We trained the Minitaur robot to walk on flat terrain (first row) in about two hours. At test time, we introduced obstacles, including a slope, wooden blocks, and steps, which were not present at training time, and the learned policy was able to generalize to the unseen situations without difficulty (other rows).

B. Results

Our method successfully learns to walk from 160k control steps, or approximately 400 rollouts. Each rollout has the maximum length of 500 steps (equivalent to 10 seconds) and can terminate early if the robot falls. The whole training process takes about two hours. Figure 7 shows the learning curve. Please refer to the supplemental video to see the learning process, the final policy, and more evaluations on different terrains.

The trained Minitaur robot is able to walk forward at a speed of 0.32m/s (equivalent to 0.8 body length per second). The learned gait swings the front legs once per cycle, while pushing against the ground multiple times with the rear legs (Figure 8a and b). Note that the learned gait is periodic and synchronized, though no explicit trajectory generator, symmetry constraint, or periodicity constraint is encoded into the system. Comparing to the default locomotion controller (trotting gait) provided by the manufacturer that walks at a similar speed, the learned gait has similar frequencies ($\sim 2\text{Hz}$) and swing amplitudes (~ 0.7 Rad), but has substantially different joint angle trajectories and foot placement. The learned gait has a much wider stance and a lower standing height. We evaluated the robustness of the trained policy against external perturbations by pushing the base of the robot backward (Figure 8c) for approximately one second, or side for around half second. Although the policy has never been trained with such perturbations, it successfully recovered and returned to a periodic normal gait for all 10 repeated tests.

In the real world, the utility of a locomotion policy hinges critically on its ability to generalize to different terrains and obstacles. Although we trained our policy only on flat terrain, as illustrated in Figure 9 (first row), we then tested it on varied terrains and obstacles (other rows). Because the soft actor-critic

method learns robust policies due to entropy maximization at training time, the policy can readily generalize to these perturbations without any additional tweaking. The robot is able to walk up and down a slope (second row), ram through an obstacle made of wooden blocks (third row), and step down stairs (fourth row) without difficulty, despite not being trained in these settings. We repeated these tests for 10 times, and the robot succeeds on all 10 trials of the slope, wooden blocks, and step down tasks.

To the best of our knowledge, this is the first example that a deep reinforcement learning algorithm successfully learns locomotion directly on a quadruped robot in the real world without any pre-training in the simulation.

VIII. CONCLUSION

We present a complete end-to-end learning system for locomotion on legged robots. The core algorithm, which is based on a dual formulation of an entropy-constrained reinforcement learning objective, can automatically adjust the temperature hyperparameter during training, resulting in a sample-efficient and stable algorithm with respect to hyperparameter settings. It enables end-to-end learning of quadrupedal locomotion controllers from scratch on a real-world robot. The walking gait emerged automatically in two hours of training without the need of prior knowledge about the locomotion tasks or the robot’s dynamic model. This success is the first step towards a new paradigm of fully autonomous real-world training for legged robots. One bottleneck of our current system is the manual reset between episodes: a person needs to manually pick up and move the robot back to the initial position. In the future work, we plan to automate this tedious and time-consuming reset process via learning [9, 23].

REFERENCES

- [1] Abbas Abdolmaleki, Jost Tobias Springenberg, Yuval Tassa, Remi Munos, Nicolas Heess, and Martin Riedmiller. Maximum a posteriori policy optimisation. *arXiv preprint arXiv:1806.06920*, 2018.
- [2] Taylor Apgar, Patrick Clary, Kevin Green, Alan Fern, and Jonathan W. Hurst. Fast online trajectory optimization for the bipedal robot cassie. In *Robotics: Science and Systems*, 2018.
- [3] Glen Berseth, Cheng Xie, Paul Cernek, and Michiel Van de Panne. Progressive reinforcement learning with distillation for multi-skilled motion control. *International Conference on Learning Representations (ICLR)*, 2018.
- [4] Gerardo Bleedt, Matthew J. Powell, Benjamin Katz, Jared Di Carlo, Patrick M. Wensing, and Sangbae Kim. MIT cheetah 3: Design and control of a robust, dynamic quadruped robot. In *IROS*, pages 2245–2252. IEEE, 2018.
- [5] Stephen Boyd and Lieven Vandenbergh. *Convex optimization*. Cambridge university press, 2004.
- [6] G. Brockman, V. Cheung, L. Pettersson, J. Schneider, J. Schulman, J. Tang, and W. Zaremba. OpenAI Gym. *arXiv preprint arXiv:1606.01540*, 2016.
- [7] Roberto Calandra, André Seyfarth, Jan Peters, and Marc Peter Deisenroth. Bayesian optimization for learning gaits under uncertainty. *Annals of Mathematics and Artificial Intelligence*, 76(1-2):5–23, 2016.
- [8] J. Di Carlo, P. M. Wensing, B. Katz, G. Bleedt, and S. Kim. Dynamic locomotion in the mit cheetah 3 through convex model-predictive control. In *2018 IEEE/RSJ International Conference on Intelligent Robots and Systems (IROS)*, pages 1–9, Oct 2018. doi: 10.1109/IROS.2018.8594448.
- [9] B. Eysenbach, S. Gu, J. Ibarz, and S. Levine. Leave no trace: Learning to reset for safe and autonomous reinforcement learning. In *6th International Conference on Learning Representations (ICLR)*, May 2018. URL <https://arxiv.org/pdf/1711.06782.pdf>.
- [10] S. Fujimoto, H. van Hoof, and D. Meger. Addressing function approximation error in actor-critic methods. In *International Conference on Machine Learning (ICML)*, 2018.
- [11] Christian Gehring, Stelian Coros, Marco Hutter, Michael Bloesch, Péter Fankhauser, Markus A Hoepflinger, and Roland Siegwart. Towards automatic discovery of agile gaits for quadrupedal robots. In *Robotics and Automation (ICRA), 2014 IEEE International Conference on*, pages 4243–4248. IEEE, 2014.
- [12] Christian Gehring, Stelian Coros, Marco Hutler, Carmine Dario Bellicoso, Huub Heijnen, Remo Diethelm, Michael Bloesch, Péter Fankhauser, Jemin Hwangbo, Mark Hoepflinger, et al. Practice makes perfect: An optimization-based approach to controlling agile motions for a quadruped robot. *IEEE Robotics & Automation Magazine*, 23(1):34–43, 2016.
- [13] Sehoon Ha, Joohyung Kim, and Katsu Yamane. Automated deep reinforcement learning environment for hardware of a modular legged robot. In *International Conference on Ubiquitous Robots (UR)*, pages 348–354. IEEE, 2018.
- [14] T. Haarnoja, H. Tang, P. Abbeel, and S. Levine. Reinforcement learning with deep energy-based policies. In *International Conference on Machine Learning (ICML)*, pages 1352–1361, 2017.
- [15] T. Haarnoja, K. Hartikainen, P. Abbeel, and S. Levine. Latent space policies for hierarchical reinforcement learning. In *International Conference on Machine Learning (ICML)*, 2018.
- [16] T. Haarnoja, V. Pong, A. Zhou, M. Dalal, P. Abbeel, and S. Levine. Composable deep reinforcement learning for robotic manipulation. In *International Conference on Robotics and Automation (ICRA)*. IEEE, 2018.
- [17] T. Haarnoja, A. Zhou, P. Abbeel, and S. Levine. Soft actor-critic: Off-policy maximum entropy deep reinforcement learning with a stochastic actor. In *International Conference on Machine Learning (ICML)*, 2018.
- [18] Nikolaus Hansen. The cma evolution strategy: a comparing review. In *Towards a new evolutionary computation*, pages 75–102. Springer, 2006.
- [19] Nicolas Heess, Srinivasan Sriram, Jay Lemmon, Josh Merel, Greg Wayne, Yuval Tassa, Tom Erez, Ziyu Wang, Ali Eslami, Martin Riedmiller, et al. Emergence of locomotion behaviours in rich environments. *arXiv preprint arXiv:1707.02286*, 2017.
- [20] P. Henderson, R. Islam, P. Bachman, J. Pineau, D. Precup, and D. Meger. Deep reinforcement learning that matters. In *Conference on Artificial Intelligence (AAAI)*. AAAI, 2018.
- [21] Marco Hutter, Hannes Sommer, Christian Gehring, Mark Hoepflinger, Michael Bloesch, and Roland Siegwart. Quadrupedal locomotion using hierarchical operational space control. *The International Journal of Robotics Research*, 33(8):1047–1062, 2014.
- [22] Marco Hutter, Christian Gehring, Dominic Jud, Andreas Lauber, C Dario Bellicoso, Vassilios Tsounis, Jemin Hwangbo, Karen Bodie, Peter Fankhauser, Michael Bloesch, et al. Anymal-a highly mobile and dynamic quadrupedal robot. In *2016 IEEE/RSJ International Conference on Intelligent Robots and Systems (IROS)*, pages 38–44. IEEE, 2016.
- [23] Jemin Hwangbo, Joonho Lee, Alexey Dosovitskiy, Dario Bellicoso, Vassilios Tsounis, Vladlen Koltun, and Marco Hutter. Learning agile and dynamic motor skills for legged robots. *Science Robotics*, 4(26), 2019. doi: 10.1126/scirobotics.aau5872.
- [24] Atil Iscen, Ken Caluwaerts, Jie Tan, Tingnan Zhang, Erwin Coumans, Vikas Sindhwani, and Vincent Vanhoucke. Policies modulating trajectory generators. In Aude Billard, Anca Dragan, Jan Peters, and Jun Morimoto, editors, *Proceedings of The 2nd Conference on Robot Learning*, volume 87 of *Proceedings of Machine Learning Research*, pages 916–926. PMLR, 29–31 Oct 2018.
- [25] Gavin D Kenneally, Avik De, and Daniel E Koditschek.

- Design principles for a family of direct-drive legged robots. *IEEE Robotics and Automation Letters*, 1(2): 900–907, 2016.
- [26] D. Kingma and J. Ba. Adam: A method for stochastic optimization. In *International Conference for Learning Presentations (ICLR)*, 2015.
- [27] Diederik P Kingma and Max Welling. Auto-encoding variational bayes. *arXiv preprint arXiv:1312.6114*, 2013.
- [28] Nate Kohl and Peter Stone. Policy gradient reinforcement learning for fast quadrupedal locomotion. In *International Conference on Robotics and Automation*, volume 3, pages 2619–2624. IEEE, 2004.
- [29] T. P. Lillicrap, J. J. Hunt, A. Pritzel, N. Heess, T. Erez, Y. Tassa, D. Silver, and D. Wierstra. Continuous control with deep reinforcement learning. *arXiv preprint arXiv:1509.02971*, 2015.
- [30] O. Nachum, M. Norouzi, K. Xu, and D. Schuurmans. Bridging the gap between value and policy based reinforcement learning. In *Advances in Neural Information Processing Systems (NeurIPS)*, pages 2772–2782, 2017.
- [31] Brendan O’Donoghue, Rémi Munos, Koray Kavukcuoglu, and Volodymyr Mnih. Pq: Combining policy gradient and q. *arXiv preprint arXiv:1611.01626*, 2016.
- [32] Xue Bin Peng, Glen Berseth, and Michiel Van de Panne. Terrain-adaptive locomotion skills using deep reinforcement learning. *ACM Transactions on Graphics (TOG)*, 35(4):81, 2016.
- [33] Jan Peters and Stefan Schaal. Policy gradient methods for robotics. In *International Conference on Intelligent Robots and Systems (IROS)*, pages 2219–2225. IEEE, 2006.
- [34] Akshara Rai, Rika Antonova, Seungmoon Song, William Martin, Hartmut Geyer, and Christopher G Atkeson. Bayesian optimization using domain knowledge on the ATRIAS biped. *arXiv preprint arXiv:1709.06047*, 2017.
- [35] Marc H Raibert. *Legged robots that balance*. MIT press, 1986.
- [36] Konrad Rawlik, Marc Toussaint, and Sethu Vijayakumar. On stochastic optimal control and reinforcement learning by approximate inference. In *Robotics: Science and Systems (RSS)*, pages 3052–3056, 2012.
- [37] J. Schulman, S. Levine, P. Abbeel, M. I. Jordan, and P. Moritz. Trust region policy optimization. In *International Conference on Machine Learning (ICML)*, pages 1889–1897, 2015.
- [38] J. Schulman, P. Abbeel, and X. Chen. Equivalence between policy gradients and soft Q-learning. *arXiv preprint arXiv:1704.06440*, 2017.
- [39] J. Schulman, F. Wolski, P. Dhariwal, A. Radford, and O. Klimov. Proximal policy optimization algorithms. *arXiv preprint arXiv:1707.06347*, 2017.
- [40] R. S. Sutton and A. G. Barto. *Reinforcement learning: An introduction*, volume 1. MIT press Cambridge, 1998.
- [41] Jie Tan, Tingnan Zhang, Erwin Coumans, Atil Iscen, Yunfei Bai, Danijar Hafner, Steven Bohez, and Vincent Vanhoucke. Sim-to-real: Learning agile locomotion for quadruped robots. In *Robotics: Science and Systems (RSS)*, 2018.
- [42] Russ Tedrake, Teresa Weirui Zhang, and H Sebastian Seung. Learning to walk in 20 minutes. In *Proceedings of the Fourteenth Yale Workshop on Adaptive and Learning Systems*, volume 95585, pages 1939–1412. Yale University New Haven (CT), 2005.
- [43] E. Todorov. General duality between optimal control and estimation. In *Conference on Decision and Control (CDC)*, pages 4286–4292. IEEE, 2008.
- [44] M. Toussaint. Robot trajectory optimization using approximate inference. In *International Conference on Machine Learning (ICML)*, pages 1049–1056. ACM, 2009.
- [45] Zhaoming Xie, Glen Berseth, Patrick Clary, Jonathan Hurst, and Michiel van de Panne. Feedback control for cassie with deep reinforcement learning. *arXiv preprint arXiv:1803.05580*, 2018.
- [46] B. D. Ziebart, A. L. Maas, J. A. Bagnell, and A. K. Dey. Maximum entropy inverse reinforcement learning. In *AAAI Conference on Artificial Intelligence (AAAI)*, pages 1433–1438, 2008.